



## Search for a large-scale anisotropy of ultra-high energy cosmic rays with the Telescope Array

M. FUKUSHIMA<sup>1</sup>, E. KIDO<sup>1</sup>, T. NONAKA<sup>1</sup>, T. OKUDA<sup>2</sup>, M. PSHIRKOV<sup>3</sup>, G. RUBTSOV<sup>4</sup>, H. SAGAWA<sup>1</sup>, A. TAKETA<sup>1</sup>, P. TINYAKOV<sup>3,4</sup>, I. TKACHEV<sup>4</sup>, FOR THE TELESCOPE ARRAY COLLABORATION

<sup>1</sup>*Institute for Cosmic Ray Research, University of Tokyo, Kashiwa, Chiba 277-8582 Japan*

<sup>2</sup>*Osaka City University, Sumiyoshi, Osaka 558-8585, Japan*

<sup>3</sup>*Université Libre de Bruxelles (ULB), bvd. du Triomphe 1050 Brussels, Belgium*

<sup>4</sup>*Institute for Nuclear Research, 60th October Anniversary prospect 7a, 117312, Moscow, Russia*

*petr.tiniakov@ulb.ac.be*

DOI: 10.7529/ICRC2011/V02/1317

**Abstract:** The correlation between the first three years of the Telescope Array surface detector data and the large-scale structure of the Universe is studied. The predicted cosmic ray flux is calculated by propagating ultra-high energy protons from sources whose distribution is derived from the complete catalog of galaxies within 250 Mpc from Earth. The flux-sampling method is used to test whether the actual data follow the model predictions. We calculate the statistical power of the flux sampling test for the case of the Telescope Array, then compare TA data with LSS model predictions with and without galactic magnetic field, and also to the isotropic distribution.

**Keywords:** Telescope Array, ultra-high energy cosmic rays, large-scale anisotropy

## 1 Introduction

Telescope Array (TA) is a hybrid detector of ultra-high energy cosmic rays (UHECRs) located in Utah, USA. It has been fully operational starting from March 2008. The ground array of TA is composed of 507 scintillator detectors covering the area of approximately 680 km<sup>2</sup>. This array is overlooked by 38 fluorescence telescopes arranged in 3 towers. In 3 years of operation, TA has accumulated the largest cosmic ray data set ever available in the Northern hemisphere.

One of the major scientific goals of TA is the study of anisotropy of UHECRs in the Northern sky. While at energies below 10<sup>18</sup> eV cosmic rays get isotropised in the Galactic magnetic field and no anisotropy is expected, the situation is different at ultra-high energies. If cosmic ray primary particles are protons as suggested by the previous studies [1, 2], their deflections in the magnetic fields at energies above 10<sup>19</sup> eV are likely to be insufficient to isotropise the flux. Therefore, any anisotropy in the cosmic-ray source distribution should manifest itself in the data.

Observation of the cutoff in the highest-energy part of the cosmic ray spectrum [3] resulting from the interactions of UHECRs with the cosmic microwave background radiation [4, 5] suggest that the UHECR propagation length at high energies becomes smaller than  $\sim 50$  Mpc. Since the matter is distributed non-uniformly at these scales, a sizeable anisotropy in the flux is expected that should correlate with

the matter distribution in the nearby Universe. In this paper we examine the TA data for the presence of such an anisotropy.

Our analysis consists of two parts: (i) calculation of the expected flux distribution and (ii) comparison of expected flux to the TA data.

First, we use the observed distribution of galaxies to infer the matter distribution at distances smaller than 250 Mpc. The matter distribution is then used to calculate the sky distribution of the expected cosmic ray flux. The latter distribution is energy dependent: the higher is the energy, the shorter is the propagation length and the smaller the region contributing to the flux. Since at smaller distances relative variations of matter density are larger, the variations of the CR flux at high energies are more pronounced. In this study we consider 3 *a priori* chosen energy thresholds which also have been used in the previous studies: 10 EeV (1 EeV = 10<sup>18</sup> eV), 40 EeV and 57 EeV.

Another important factor that affects the calculation of the CR flux is deflections in the magnetic fields. We use two different methods of taking the deflections into account. Random deflections caused by the extragalactic magnetic field and by the turbulent part of the Galactic field can be taken into account by smearing each source within certain angular scale  $\theta_s$ . The smearing reduces the variations of the flux, so that in the limit of large  $\theta_s$  the flux becomes isotropic. In this analysis we consider  $\theta_s$  as a free parameter.

In the case of deflections by the regular component of the Galactic magnetic field, smearing may become a poor approximation if the deflection angles is larger than  $10 - 15^\circ$ . In this case the deflections in the regular Galactic magnetic field should be taken into account explicitly in the calculation of the expected flux, which requires a reasonable knowledge of the GMF.

In the second part of the analysis the expected flux, which is a function of the smearing angle and also the parameters of GMF if the latter is taken into account explicitly, is compared to the TA data. This allows to rule out model parameters that do not reproduce the observed cosmic ray distribution. The comparison is performed by the flux-sampling method [6] (see Sect. 3.1 for more details).

## 2 Data

This analysis is based on the TA data collected during 3 years of the surface detector operation in the period from March 2008 till March 2011. With the zenith angle cut of  $45^\circ$ , this data set contains 809 events with energies higher 10 EeV, 46 events with energies higher than 40 EeV and 19 events with energies higher than 57 EeV. Above 10 EeV, the angular resolution of TA events is better than  $1.5^\circ$ , while the energy resolution is about 20%.

Comparison of the data to the expected flux distribution requires good knowledge of the exposure function. In the case of the TA surface detector, and for the data set with energies  $E > 10$  EeV, the exposure is well approximated by the geometrical one. The approximation is expected to be better at higher energies.

Fig. 1 shows the comparison between the distributions in the declination (left column) and right ascension (right column) of the events in the Monte-Carlo simulations based on the geometrical exposure (red line) and in the data (blue line) with energy thresholds  $E > 10$  EeV,  $E > 40$  EeV and  $E > 57$  EeV (top, middle and bottom rows, respectively). The  $E > 10$  EeV and  $E > 40$  EeV sets are compatible with geometrical exposure. This also indicates the absence of strong deviation from isotropy in these sets. The highest-energy set has the distribution in the right ascension which is mildly incompatible with the corresponding distribution of the simulated set: the probability that the two distributions are the same is 4% according to the Kolmogorov-Smirnov (KS) test.

The matter distribution in the nearby Universe is inferred from the galaxy catalogs containing the redshift information, namely, the 2MASS Galaxy Redshift Catalog (XSCz) [7] that is derived from the 2MASS Extended Source Catalog (XSC). This catalog provides the most accurate information about 3D galaxy distribution to date. To map the flux distribution we use galaxies brighter than  $m = 12.5$  in the K-band which are situated at distances  $5 \text{ Mpc} < d < 250 \text{ Mpc}$  from the Earth. There are 109 408 objects satisfying these conditions in the catalog.

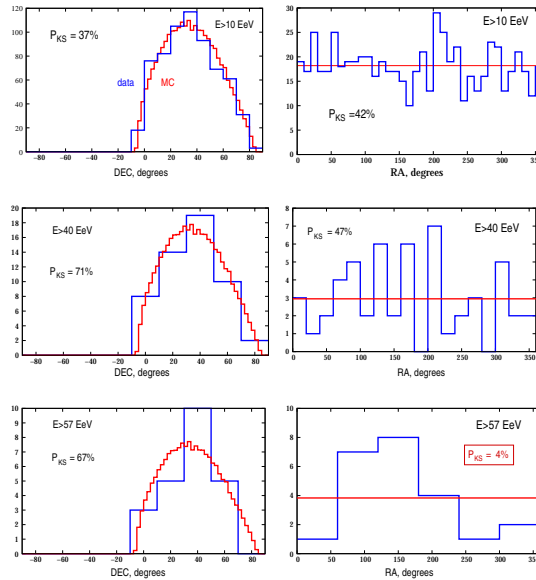


Figure 1: Comparison between the data (blue line) and the geometrical exposure simulations (red line) at energies 10 EeV, 40 EeV and 57 EeV (top, middle and bottom rows, respectively). Plots show the distribution of events in declination (right column) and right ascension (left column). The compatibility of the two distributions by the Kolmogorov-Smirnov test is given as  $P_{KS}$ .

## 3 Method

### 3.1 Calculation of the model flux distribution

The distribution of the expected flux over the sky is generated as follows. First, galaxies in the flux-limited sample described above are weighted to compensate for a progressive incompleteness of the flux-limited sample at large distances. The weighting algorithm is described in Ref. [8]. It allows one to use most efficiently the information on the matter distribution contained in the catalog.

Then all galaxy weights are corrected for the attenuation of the cosmic ray flux due to redshift, interactions with CMB and other photon backgrounds. The primary particles are assumed to be protons. The injection spectrum at the source is taken to be a power-law with the index of 2.2, which is consistent with the observed CR spectrum.

At the last stage the contributions of individual galaxies to the flux in a given point are added according to their weights and angular distances to that point. The dependence on the distance is taken Gaussian with the width equal to  $\theta_s$ , so that only galaxies within the angular distance of a few  $\theta_s$  from the given point contribute significantly.

Finally, a uniform component is added representing cumulative contribution of sources beyond the distance of 250 Mpc. The relative strength of the uniform component is calculated in the same way as the attenuation factors for

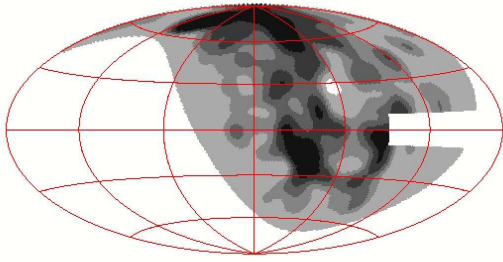


Figure 2: Sky map of expected flux at  $E > 57$  EeV (Galactic coordinates). The region  $|b| < 10^\circ$ ,  $|l| < 90^\circ$  is excluded from the analysis. The smearing angle is  $6^\circ$ .

individual galaxies. After adding all the contributions, the flux is multiplied by the exposure function of the TA detector. Further details of the flux calculation can be found in Refs.[6, 8, 1].

The flux map at the energy threshold of  $E > 57$  EeV calculated as described above is shown in Fig. 2. The rectangular region around the Galactic center  $|b| < 10^\circ$ ,  $|l| < 90^\circ$  is cut from the analysis because of the incompleteness of the underlying galaxy catalog in this region. Dark areas represent the regions of larger flux. They correspond to matter overdensities in the nearby Universe.

### 3.2 Flux-sampling test

The flux-sampling test [6] is designed to compare the sky distribution of the observed cosmic ray events to the expected cosmic ray flux. It is based on the following idea. A set of cosmic ray events defines a set of flux *values* which are read off at the corresponding directions on the sky. In this sense the set of cosmic rays samples the flux map. The resulting set of flux values characterizes, indirectly, the space distribution of cosmic rays in the set: for instance, if cosmic rays come preferentially from regions of high flux, the set of flux values will contain more higher values. If two sets of cosmic rays are drawn from the same distribution, the corresponding two distributions of flux values must agree. The compatibility of these distributions may be tested by the KS test.

In the actual test one uses the flux map that corresponds to the matter distribution. The hypothesis to be tested is that the cosmic ray sources follow the distribution of matter (we will refer to it as the LSS hypothesis). One of the cosmic ray sets is generated according to this hypothesis. Another set is the real data. The result of the KS test gives the probability (more precisely, p-value) that the two sets are drawn from the same distribution. Low p-values, therefore, indicate incompatibility between the data and the LSS hypothesis. In this analysis we choose an *a priori* confidence level (CL) of 95%, meaning that if the p-value comes out smaller than 0.05, the data are incompatible with the LSS hypothesis at the 95% CL.

An important characteristics of a statistical test is its discriminative power which shows the ability of a test to distinguish two hypotheses (powers close to 1 correspond to high discriminative ability). We have calculated the statistical power of the flux sampling test to discriminate between the LSS hypothesis and isotropy for the three energy cuts of  $E > 10$  EeV,  $E > 40$  EeV and  $E > 57$  EeV, and smearing angles varying from 2 to 14 degrees. The results of the simulations are presented in Fig. 3.2. Different curves show statistical power for different number of events. As can be seen from the figure, the statistical power of the test in distinguishing the two models decreases with increasing smearing angle. This is expected since as the smearing angle increases, the predictions of the LSS and isotropy models become more and more alike. Another observation is that at the current number of events (35 at  $E > 40$  EeV and 15 at  $E > 57$  EeV) the statistical power is below 50% for all smearing angles.

### 3.3 Account for the Galactic magnetic field

At low energies cosmic ray deflections in the Galactic magnetic field may be too large to be accounted for by introducing the smearing angle. Indeed, recent data on Faraday rotations of extragalactic sources indicate that the Galactic magnetic field contains a halo component of a substantial strength [9]. This component may lead to cosmic ray deflections that are larger than was typically thought before.

In this case the flux map has to be corrected for GMF before it is compared to the data. The correction can be done by back-tracing of anti-protons: the corrected value in a given direction is simply the original (not corrected for GMF) flux value in the direction obtained by tracing back an anti-proton of same energy. The example of the corrected flux map for the energy threshold  $E > 40$  EeV is shown in Fig.4.

## 4 Results of the tests and conclusions

The results of the statistical tests with the current TA data will be presented at the conference.

### Acknowledgements

The Telescope Array experiment is supported by the Japan Society for the Promotion of Science through Grants-in-Aid for Scientific Research on Specially Promoted Research (21000002) “Extreme Phenomena in the Universe Explored by Highest Energy Cosmic Rays”, and the Inter-University Research Program of the Institute for Cosmic Ray Research; by the U.S. National Science Foundation awards PHY-0307098, PHY-0601915, PHY-0703893, PHY-0758342, and PHY-0848320 (Utah) and PHY-0649681 (Rutgers); by the National Research Foundation of Korea (2006-0050031, 2007-0056005, 2007-0093860, 2010-0011378, 2010-0028071, R32-10130); by

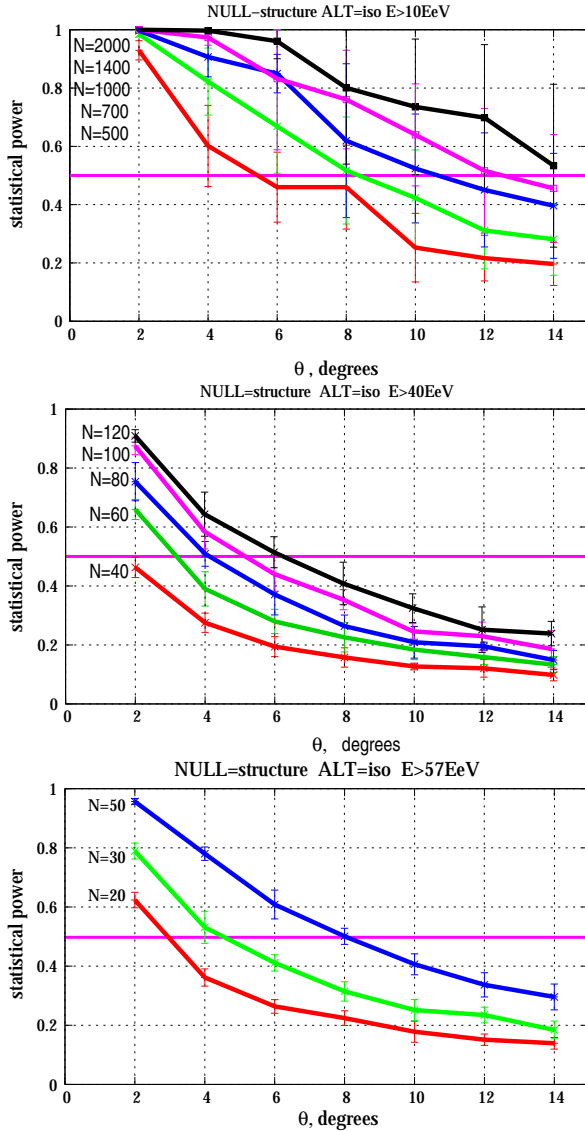


Figure 3: The statistical power of the flux sampling test at the energy threshold of 10 EeV, 40 EeV and 57 EeV as a function of the smearing angle. Different curves correspond to different number of events, as indicated on the plot. Gray region shows expected deflections in the Galactic magnetic field assuming primary protons.

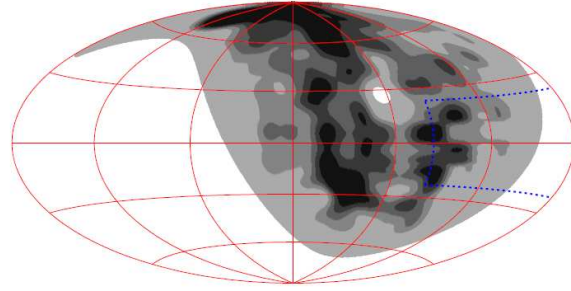


Figure 4: Sky map of the flux expected in the LSS model corrected for the Galactic magnetic field. Dashed line marks the region where the flux may be affected by the incompleteness of the galaxy catalog around the Galactic Center.

the Russian Academy of Sciences, RFBR grants 10-02-01406a and 11-02-01528a (INR), IISN project No. 4.4509.10 and Belgian Science Policy under IUAP VI/11 (ULB). The foundations of Dr. Ezekiel R. and Edna Wattis Dumke, Willard L. Eccles and the George S. and Dolores Dore Eccles all helped with generous donations. The State of Utah supported the project through its Economic Development Board, and the University of Utah through the Office of the Vice President for Research. The experimental site became available through the cooperation of the Utah School and Institutional Trust Lands Administration (SITLA), U.S. Bureau of Land Management and the U.S. Air Force. We also wish to thank the people and the officials of Millard County, Utah, for their steadfast and warm support. We gratefully acknowledge the contributions from the technical staffs of our home institutions and the University of Utah Center for High Performance Computing (CHPC).

## References

- [1] R. U. Abbasi, et al., *Astrophys. J. Lett.* **713**, L64–L68 (2010).
- [2] Y. Tameda (2010), prepared for International Symposium on the Recent Progress of Ultra-high Energy Cosmic Ray Observation (UHECR2010), Nagoya, JAPAN Dec.10-12.
- [3] R. Abbasi, et al., *Phys. Rev. Lett.* **100**, 101101 (2008).
- [4] K. Greisen, *Phys. Rev. Lett.* **16**, 748–750 (1966).
- [5] G. T. Zatsepin, and V. A. Kuzmin, *JETP Lett.* **4**, 78–80 (1966).
- [6] H. B. J. Koers, and P. Tinyakov, *JCAP* **0904**, 003 (2009).
- [7] We thank T. Jarrett for providing us with the preliminary version of this catalog.
- [8] H. B. J. Koers, and P. Tinyakov, *Mon. Not. Roy. Astron. Soc.* **399**, 1005–1011 (2009).
- [9] M. S. Pshirkov, P. G. Tinyakov, P. P. Kronberg, K. J. Newton-McGee, arXiv:1103.0814.